AN ABSTRACT OF THE THESIS OF

Bartlett Knapp Smith for the degree of Master of Science

in Atmospheric Sciences presented on May 30, 1979

Title: Dynamics of a Differentially-Heated Geophysical Boundary Layer

Abstract approved Redacted for privacy

Larry J. Mahrt

An analytical two-layer model consisting of a time-dependent stratified boundary layer topped by stratified free flow is developed in order to study atmospheric boundary layer production of vertical motion. To avoid use of a constant eddy viscosity, the boundary layer equations are layer-integrated over a fixed depth, and surface stress is parameterized using a linearized drag law.

For flows driven by periodic, differential surface heating, it is found that the influence of accelerations, stratification, and friction are to concentrate the maximum convergence near a preferred latitude. The preferred horizontal length scale for boundary layer production of vertical motion increases with boundary layer stratification and decreases with distance from the preferred latitude.

DYNAMICS OF A DIFFERENTIALLY-HEATED GEOPHYSICAL BOUNDARY LAYER

by

Bartlett Knapp Smith

A THESIS

submitted to

Oregon State University

in partial fulfillment of
the requirements for the
degree of

Master of Science

Completed June 1979

Commencement June 1980

APPROVED:

Redacted for privacy

Associate Professor of Atmospheric Sciences
in charge of major

Redacted for privacy

Chairman of the Department of Atmospheric Sciences

Redacted for privacy

Dean of Graduate School

Date thesis is presented May 30, 1979

Typed by Margot Lillestol for Bartlett K. Smith

ACKNOWLEDGEMENTS

I wish to express my sincere gratitude to my major professor, Dr. Larry Mahrt for his time, patience, and good-natured guidance throughout my masters program.

I am also very grateful to Ms. Margot Lillestol for typing the final manuscript.

Finally, a very special thanks to my parents, my wife Ann, and my daughter Alexis for their many sacrifices, and for all the kindness and support they've extended throughout this endeavor.

This research was supported by Research Grant ATM 76-81908 and ATM 77-07623, Atmospheric Sciences Section, National Science Foundation.

TABLE OF CONTENTS

LIST OF ILLUSTRATIONS

DYNAMICS OF A DIFFERENTIALLY-HEATED GEOPHYSICAL BOUNDARY LAYER

I. INTRODUCTION

A. Importance of the Problem

Production of vertical motion and associated convergence of moisture is important to many types of atmospheric phenomena. Often the processes of cloud formation, latent heat release, precipitation, and pressure adjustments are all directly coupled to boundary layer convergence on both meso-and synoptic-scale motions. These phenomena can significantly influence the dynamics of the overlying frictionless flow. In turn, the adjusting flow above the boundary layer extends its influence downward through the hydrostatic pressure field, altering the dynamics associated with the production of vertical motion. Therefore, understanding the mechanisms which promote or inhibit boundary layer convergence is an important requisite to an understanding of the dynamics of many atmospheric flows.

B. Review of Earlier Studies

The most fundamental analytical study of boundary layer convergence is the classical Ekman solution in which the boundary layer flow is treated as a balance between a specified pressure gradient force, the Coriolis force, and the force due to turbulent stress divergence. Solution of this system relates the stress to the local shear through a constant eddy viscosity assumption. The resulting vertical motion field is proportional to the relative geostrophic vorticity and the Ekman layer depth (Charney and Eliassen, 1949). This vertical motion induces pressure adjustments which

act to destroy geostrophic vorticity as in spin-down(up) (Greenspan and Howard, 1963).

Improvements to this theory have been primarily aimed at including the effects of accelerations and stratification on frictionally induced convergence. Most studies to date have considered their influences independently.

In the steady-state boundary layer (Stommel and Veronis, 1957; Barcilon and Pedlosky, 1967; Leetma, 1971; Kuo, 1973) where vertical advection of temperature balances turbulent heat transport, the vertical motion is linearly proportional to the inverse of the stratification. Stratification may also inhibit vertical motion through pressure adjustments associated with adiabatic cooling in non-steady flows.

Investigations by Young (1973) and Mahrt (1974) showed that in the presence of an intensifying pressure gradient, accelerations act to increase cross-isobar flow and vertical motion at a given latitude. Kuo (1973) pointed out that accelerations could reduce the influence of stratification if the time scale for temperature diffusion is large compared to the local time rate of change of temperature.

Greenspan (1968) noted that the periodic time-dependent Ekman solutions have an infinite boundary layer depth at the latitude where the local Coriolis parameter equals the oscillation frequency (critical latitude). The critical latitude effect was also discussed by Holton et al. (1971), Chang (1973), and Kuo (1975) who found that the vertical motion field associated with synoptic scale wave disturbances is a maximum in a region where opposing local accelerations are of magnitude comparable to the Coriolis accelerations.

Interactions between accelerations and stratification have received only limited attention. Holton (1965) and Mahrt and Park (1976) found that the spin-up(down) time for stratified frictionless flow was reduced from the homogeneous fluid result of Greenspan and Howard (1963). Both authors neglected pressure adjustments within the boundary layer. In a study including local accelerations and boundary layer pressure adjustments, Kuo (1975) found that boundary layer stratification greatly reduced the concentration of vertical motion near the critical latitude for periodic, synoptic scale disturbances. Park and Mahrt (1978) considered the influence of accelerations and stratification on frictionally induced convergence for a range of time scales. Their solutions reduced to functions of m and $\hat{\omega}$, which are respectively, the product of an Ekman number times a stratification parameter and the ratio between the forcing (surface temperature variation) frequency and the local Coriolis parameter. They found increasing m reduced vertical motion for a fixed amount of thermal forcing and fixed $\hat{\omega}$. Accelerations might inhibit or enhance convergence depending on the values of m and $\hat{\omega}$.

Stratification and pressure adjustments within the boundary layer are almost always neglected in time-dependent boundary layers. They are thought to be of secondary importance to pressure adjustments in the much deeper overlying frictionless flow. Kuo (1975) and Park and Mahrt (1978) found that this approximation breaks down in boundary layers with strong stratification, as might result from surface radiative cooling in the nocturnal boundary layer, if the scale of the forcing is sufficiently small. Many geophysical problems such as the urban heat island and sea-breeze circulations occur at small enough scales to make boundary layer pressure

adjustments important even when stratification is small.

Most analytical studies of boundary layer dynamics parameterize turbulent transport with constant eddy viscosity, which is of uncertain validity when applied to geophysical flows. In the daytime mixed-layer, for example, the eddy viscosity may become locally infinite or negative. An alternative method is to layer-integrate the boundary layer equations over a specified depth as in Geisler and Kraus (1969), Lavoie (1972), and Mahrt (1974). Then values of stress are required only at the surface and boundary layer top which in turn can be related to the mean structure through similarity parameterization. Some drawbacks to this approach are the loss of vertical structure in the boundary layer and the arbitrariness of the assigned constant boundary layer depth, which in reality might depend on several parameters in the problem, and vary significantly in time.

C. The Present Study

In this paper we will study boundary layer convergence using the layer-integrated approach with simplified similarity theory and thus avoid use of the constant eddy viscosity assumption. In order to include height variations in stratification, we will consider a two-layer model in which turbulent transports are confined to the lower vertically-averaged layer. This approach allows inclusion of pressure adjustments in the boundary layer and aloft. Vertical variation of stratification is particularly significant in the case of the mixed-layer, where stratification is much weaker in the boundary layer than aloft, and on clear nights where stratification in the boundary layer is much stronger than aloft.

The methodology discussed in this paper is general and should be quite

adaptable to different types of forcing. As an example, we chose to examine vertical motion forced by differential surface heating as would occur in horizontal inhomogeneity of surface properties as in the sea-breeze and heat island problems. Alternative approaches might be to force the flow through an imposed pressure field or specified initial conditions.

As in any forced linear system, the solution can be characterized as the sum of the homogeneous solution and the particular solution. In Sec. II a differential equation describing vertical motion produced by boundary layer convergence is derived from basic equations. In Sec. III we examine the unforced vertical motion, or homogeneous response, whose character is determined by the differential equation for the unforced system and the initial conditions. The effect of initial conditions is discussed only with regard to spin-down. In Sec. IV the forced vertical motion is discussed with emphasis on the influence of drag coefficient, accelerations, stratification, and the scale of the forcing.

II. GOVERNING EQUATIONS

For small amplitude (small Rossby number), Boussinesq, adiabatic, hydrostatic flow, the governing equations for the time-averaged flow are:

$$\frac{\partial \bar{u}}{\partial t} - f\bar{v} = -\frac{1}{\rho_s}\frac{\partial \bar{p}}{\partial x} - \frac{\partial}{\partial z}\overline{u'w'} \tag{1}$$

$$\frac{\partial \bar{v}}{\partial t} + f\bar{u} = -\frac{1}{\rho_s}\frac{\partial \bar{p}}{\partial y} - \frac{\partial}{\partial z}\overline{v'w'} \tag{2}$$

$$\frac{\partial \bar{p}}{\partial z} = \frac{\rho_s}{\theta_s} g\,\bar{\theta} \tag{3}$$

$$\frac{\partial \bar{\theta}}{\partial t} + \bar{w}\frac{d\theta_s}{dz} = -\frac{\partial}{\partial z}\overline{\theta'w'} \tag{4}$$

$$\frac{\partial \bar{u}}{\partial x} + \frac{\partial \bar{v}}{\partial y} + \frac{\partial \bar{w}}{\partial z} = 0 \tag{5}$$

where each field has been written as

$$\phi(x,y,z,t) = \phi'(x,y,z,t) + \bar{\phi}(x,y,z,t) + \phi_s(z)$$

The subscript "s" refers to the height dependent basic state value for the undisturbed flow, the "overbar" to the non-turbulent (time-averaged) part of the disturbed flow, and the "prime" refers to the turbulent deviation from this time average. We partition dependence on independent variables as follows:

$$[\bar{u},\bar{v}] = [u(z,t),\ v(z,t)] \sin x/L \tag{6}$$

$$[\bar{w},\bar{p},\bar{\theta}] = [w(z,t),\ p(z,t),\ \theta(z,t)] \cos x/L$$

$$[\overline{u'w'},\ \overline{v'w'}] = [\overline{\overline{u'w'}}(z,t),\ \overline{\overline{v'w'}}(z,t)] \sin x/L$$

$$\overline{\theta'w'} = \overline{\overline{\theta'w'}}(z,t) \cos x/L$$

where L is the horizontal length scale of the imposed forcing which might be, for example, differential surface heating. We assume the flow is locally invariant in the y direction. This partitioning filters out propagating waves by requiring any forced or unforced oscillation to be spatially fixed, allowing only standing wave type of solutions. Substituting these expressions into the governing equations (1)-(5), produces the following system of equations for the complex amplitudes which are height and time-dependent.

$$\frac{\partial u(z,t)}{\partial t} - fv(z,t) = \frac{p(z,t)}{\rho_s L} - \frac{\partial}{\partial z}\overline{\overline{u'w'}}(z,t) \tag{7}$$

$$\frac{\partial v(z,t)}{\partial t} + fu(z,t) = -\frac{\partial}{\partial z}\overline{\overline{v'w'}}(z,t) \tag{8}$$

$$\frac{\partial p(z,t)}{\partial z} = \frac{\rho_s g}{\theta_s}\,\theta(z,t) \tag{9}$$

$$\frac{\partial \theta(z,t)}{\partial t} + w(z,t)\,\theta_s\,\frac{N^2}{g} = -\frac{\partial}{\partial z}\overline{\overline{\theta'w'}}(z,t) \tag{10}$$

$$\frac{u(z,t)}{L} + \frac{\partial w(z,t)}{\partial z} = 0 \tag{11}$$

$$N^2 \equiv \frac{g}{\theta_s}\,\frac{d\theta_s}{dz} = \text{Brunt - Väisälla frequency}$$

The boundary layer, in this model, extends from the top of the surface layer, z=0, to a specified constant height h, and is characterized by Brunt-Väisälla frequency N_B. In most geophysical flows, the boundary layer height is a complicated function of time. For the purpose of this study, h represents the maximum boundary layer height: the uppermost extent of turbulent fluxes associated with surface roughness and heating. In the overlying

air, extending from z=h to the top of the atmosphere and characterized by Brunt-Väisälä frequency N_f, turbulent fluxes are neglected compared to adiabatic temperature changes due to vertical motion in the presence of stratification.

Vertical integration of the boundary layer equations (7)-(11) over the depth h produces a system of equations for the boundary layer averaged fields, designated by $\overline{(\ )}^h$ where

$$\overline{(\ )}^h \equiv \frac{1}{h}\int_0^h (\ )\, dz \tag{12}$$

Since the scale height for the basic state fields θ_s and ρ_s is typically much larger than the boundary layer height, we can replace the height-dependent undisturbed fields, to a good approximation, with their layer-averaged values θ_o and ρ_o.

Neglecting turbulent fluxes at the boundary layer top and layer-integrating equations (7)-(11) we obtain:

$$\frac{d\bar{u}^h}{dt} - f\bar{v}^h = \frac{\bar{p}^h}{\rho_o L} + \frac{(\overline{u'w'})_o}{h} \tag{13}$$

$$\frac{d\bar{v}^h}{dt} + f\bar{u}^h = \frac{(\overline{v'w'})_o}{h} \tag{14}$$

$$\frac{p(h,t) - p(o,t)}{h} = \frac{\rho_o}{\theta_o}\, g\, \bar{\theta}^h \tag{15}$$

$$\frac{d\bar{\theta}^h}{dt} + \bar{w}^h \frac{\theta_o}{g} N_B^2 = \frac{(\overline{\theta'w'})_o}{h} \tag{16}$$

$$\frac{\bar{u}^h}{L} + \frac{w(h,t)}{h} = 0 \tag{17}$$

Vertical motion at the surface layer top is neglected compared to w(h). The subscript "o" designates fluxes evaluated at the top of the surface layer. Surface stress will be parameterized using a linearized drag law,

$$\overline{\overline{(u'w')}}_o = - C_D V \, (\bar{u}^h \cos\eta - \bar{v}^h \sin\eta) \tag{18}$$

$$\overline{\overline{(v'w')}}_o = - C_D V \, (\bar{v}^h \cos\eta + \bar{u}^h \sin\eta) \tag{19}$$

where C_D is a specified constant drag coefficient, V is a scale velocity, and η is the specified constant angle between the surface wind and the layer mean wind. In the present problem the scale velocity depends on the surface heat flux through the thermal wind relationship:

$$V \sim |v_g(o) - v_g(h)| = \frac{h}{L} \frac{g}{f} \left| \frac{\bar{\theta}^{-h}}{\theta_o} \right| \sim \frac{g}{\omega f \theta_o} \frac{|Q_o|}{L} \tag{20}$$

where ω and Q_o are respectively, the frequency and the complex amplitude of the surface heat flux,

$$\overline{\overline{(\theta'w')}}_o = Q_o e^{-i\omega t} \tag{21}$$

A restrictive assumption is that the boundary layer depth remains relatively constant so that definition of an upperbound to the boundary layer is never too far from the actual boundary layer top. We therefore, must require that the upward advective time scale be much longer than the diffusive turbulent time scale:

$$\frac{h}{\bar{w}(h)} >> \frac{h}{C_D V} \quad \text{or} \quad C_D >> \frac{\bar{w}(h)}{V} \sim \frac{h}{L}$$

In order to close the layer-averaged system of equations (13)-(19), we

introduce the boundary layer structure parameters r and s which relate layer-averaged pressure and vertical motion to values at the boundary layer top and bottom.

$$\tilde{p}^h = \frac{rp(h,t) + p(o,t)}{r+1} \tag{22}$$

$$\tilde{w}^h = \frac{s}{s+1} w(h,t) \tag{23}$$

If pressure adjustments in the boundary layer are neglected the introduction of s is not required. These layer-averaged values correspond to general profiles of the form

$$p(z,t) = p(h,t) + (1-z/h)^r [p(o,t) - p(h,t)] \tag{24}$$

$$w(z,t) = w(h,t) [1 - (1-z/h)^s] \tag{25}$$

For example, a well-mixed layer would assume values of (r,s)=1, while exponential profiles with e^{-1} folding height h in θ and u as in Ekman flow correspond to (r,s)=1.4. The structure parameters are not very sensitive to different theoretical profiles nor will the dynamics of different flow situations turn out to be very sensitive to the structure parameters. In fact, the discussion of physical interactions presented here do not require determination of these structure functions. They are merely convenient for mathematical completeness.

Combining equations (13)-(19) and (22)-(23) results in a single equation for pressure and vertical motion at the boundary layer top.

$$\left(\left[f + \frac{C_D V}{h} \sin\eta\right]^2 + \left[\frac{d}{dt} + \frac{C_D V}{h} \cos\eta\right]^2\right) \frac{d}{dt} w(h,t)$$

$$+ \frac{s}{(s+1)(r+1)} \frac{h^2}{L^2} N_B^2 \left[\frac{d}{dt} + \frac{C_D V}{h} \cos\eta\right] w(h,t)$$

$$+ \frac{h}{\rho_o L^2}\left(\frac{d}{dt} + \frac{C_D V}{h}\cos\eta\right)\frac{d}{dt}\,p(h,t)$$

$$= \frac{h}{L}\,\frac{g}{(r+1)\theta_o}\left(\frac{d}{dt} + \frac{C_D V}{h}\cos\eta\right)\,\frac{(\overline{\overline{\theta' w'}})_o}{L} \qquad (26)$$

Equation (26) describes boundary layer production of vertical motion as a function of forcing, due to surface heating and due to the pressure field induced upon the boundary layer by the frictionless flow aloft.

In the steady-state limit, equation (26) reduces to the layer-averaged thermodynamic equation for steady boundary layer flow.

$$\frac{s}{(s+1)}\,w(h) = \overset{-h}{w} = \frac{g}{\theta_o}\,\frac{(\overline{\overline{\theta' w'}})_o}{N_B^2\,h}$$

As in Stommel and Veronis (1957), vertical motion is linearly proportional to the inverse of stratification.

In order to retain the dynamical coupling between the frictionless flow and the time-dependent boundary layer, we will calculate pressure adjustments in the flow aloft due to boundary layer production of vertical motion. These pressure adjustments aloft are, in turn, hydrostatically induced upon the boundary layer.

Neglecting the turbulent fluxes in equations (7)-(11), we get the equations for the frictionless flow above the boundary layer ($z \geq h$), with variables subscripted by "f".

$$\frac{\partial u_f}{\partial t} - f v_f = \frac{p_f}{\rho_s L} \qquad (27)$$

$$\frac{\partial v_f}{\partial t} + f u_f = 0 \qquad (28)$$

$$\frac{\partial p_f}{\partial z} = \frac{\rho_s g}{\theta_s} \theta_f \tag{29}$$

$$\frac{\partial \theta}{\partial t} + w_f \frac{\theta_s N^2}{g} f = 0 \tag{30}$$

$$\frac{u_f}{L} + \frac{\partial w_f}{\partial z} = 0 \tag{31}$$

In this layer, where turbulent f luxes are neglected, vertical motion in the presence of stratification drives temperature and pressure adjustments. Combining equations (27), (28), and (31) produces an equation which relates pressure adjustments to convergence in the frictionless layer:

$$\left(\frac{\partial^2}{\partial t^2} + f^2\right) \frac{\partial}{\partial z} w_f(z,t) = - \frac{1}{\rho_s L^2} \frac{\partial}{\partial t} p_f(z,t) \tag{32}$$

If pressure adjustments in the free flow are confined to a depth much shallower than the scale height for θ_s and ρ_s, the basic state can be approximated with constant values θ_o and ρ_o. By evaluating the depth scale in equation (35) we can see that this restriction will be valid in mesoscale and smaller scale flows. Combining equations (29), (30), and (32) leads to a single equation for pressure or vertical motion.

$$\left\{ \left(\frac{\partial^2}{\partial t^2} + f^2\right) \frac{\partial^2}{\partial z^2} - \frac{N_f^2}{L^2} \right\} \left[p_f(z,t),\ w_f(z,t) \right] = 0 \tag{33}$$

Since we are interested in the coupling mechanisms between the time-dependent boundary layer and the frictionless flow, we will consider only the case in which the boundary layer and overlying flow oscillate and decay with the same frequency and time constant. Pressure adjustments in the frictionless flow are then due to boundary layer production of vertical motion

alone, and exclude adjustments due to oscillating free modes not associated with boundary layer convergence.

The two-layer model is a coupled dynamical system which oscillates in response to the time-dependent forcing (differential heating); in addition, it may respond in any one or combination of its unforced modes. The forced response due to surface heating as in equation (21), is obtained by solving equations (26) and (33). We assume continuity in pressure and vertical motion at the interface z=h, and invoke periodic time dependence on pressure and vertical motion. Before examining the amplitude and phase of the forced response, we will look at the unforced modes for the two-layer system.

III. UNFORCED MODES

To examine the unforced modes we assume a general time-dependence of the form

$$\left[p_f(z,t), w_f(z,t)\right] = \left[p_f(z), w_f(z)\right] e^{\alpha t} \tag{34}$$

Normally, the frequency α is complex, leading to both oscillating and damped responses. From equation (33), the height-dependent amplitudes in the free flow ($z \geq h$) are

$$\left[p_f(z),\ w_f(z)\right] = \left[p(h),\ w(h)\right] \exp\left\{ \frac{-N_f}{L} \frac{(z-h)}{\sqrt{f^2+\alpha^2}} \right\} \tag{35}$$

Substituting the expressions for p_f and w_f into equation (32) and combining this with the unforced $\left(\overline{(\theta' w')}_o = 0\right)$ boundary layer equation (26), we get a sixth order polynomial in α,

$$\left[\left(f + \frac{C_D V}{h} \sin\eta\right)^2 + \left(\alpha + \frac{C_D V}{h} \cos\eta\right)^2\right] \alpha$$

$$+ \frac{s}{(s+1)(r+1)} \frac{h^2}{L^2} N_B^2 \left(\alpha + \frac{C_D V}{h} \cos\eta\right)$$

$$+ \frac{h}{L} N_f \sqrt{f^2 + \alpha^2} \left(\alpha + \frac{C_D V}{h} \cos\eta\right) = 0 \tag{36}$$

Equation (36) is a characteristic equation; its six roots represent the possible free oxcillation and dampening modes in the two-layer system. Dividing by f^3 transforms equation (36) into non-dimensional form:

$$\left[(1 + \hat{C}_D \sin\eta)^2 + (\hat{\alpha} + \hat{C}_D \cos\eta)^2\right] \hat{\alpha} \tag{37}$$

$$+ A^2 \hat{B}^2 (\hat{\alpha} + \hat{C}_D \cos\eta) + \hat{B} \sqrt{1 + \hat{\alpha}^2}\ (\hat{\alpha} + \hat{C}_D \cos\eta) = 0$$

$\hat{\alpha} \equiv \alpha/f$ = dimensionless complex frequency

$\hat{B} \equiv \frac{hN_f}{Lf}$ = free flow stratification parameter

$\hat{C}_D \equiv \frac{C_D V}{hf}$ = scaled drag coefficient

$A \equiv \sqrt{\frac{s}{(s+1)(r+1)}}$ N_B/N_f = boundary layer stratification parameter

The relative size of the non-dimensional parameters $\hat{B}$, $\hat{C}_D$, and A, determines the nature of the unforced modes subject to the initial conditions imposed upon the flow. The scaled drag coefficient $\hat{C}_D$ can be interpreted as the ratio between the inertial time scale and the time scale for turbulent diffusion through the boundary layer. For midlatitude flows with weak friction, for example, we expect $\hat{C}_D << 1$. The stratification parameter $\hat{B}$ dictates the "strength" of pressure adjustments in the free flow. When $\hat{B}$ is small, pressure adjustments are small, that is, stratification is weak or convergence is spread out over a large horizontal scale. The value of A represents the relative importance of pressure adjustments in the boundary layer compared to pressure adjustments aloft. For a well-mixed boundary layer A=0, but in a nocturnal boundary with strong radiative cooling near the surface, A is normally greater than one.

The roots to equation (37) can be calculated numerically through successive approximations for given values of the flow parameters. An alternative approach is to expand $\hat{\alpha}$ in some small parameter and investigate the assymptotic solution to equation (37) in terms of the variables $\hat{B}$, $\hat{C}_D$, and A. For example, if the two layers are weakly stratified or if the aspect ratio is small, we could expand $\hat{\alpha}$ in the small parameter $\hat{B}$.

$$\hat{\alpha} = \alpha_o + \hat{B}\alpha_1 + \hat{B}^2\alpha_2 + \cdots \qquad (38)$$

Substituting this expression into the polynomial equation (37) and taking the limit $\hat{B} \to 0$, reduces the form to a cubic in α_o.

$$\left[(1 + \hat{C}_D \sin\eta)^2 + (\alpha_o + \hat{C}_D \cos\eta)^2\right] \alpha_o = 0 \qquad (39)$$

The three zero order roots are:

$$\alpha_o = 0 \qquad (40.a)$$

$$\alpha_o = -\hat{C}_D \cos\eta - i\,(1 + \hat{C}_D \sin\eta) \qquad (40.b)$$

$$\alpha_o = -\hat{C}_D \cos\eta + i\,(1 + \hat{C}_D \sin\eta) \qquad (40.c)$$

The root $\alpha_o = 0$ represents the zero order stationary state in which the pressure gradient force, Coriolis, and frictional forces are in balance. Heating due to turbulent heat flux is balanced by adiabatic cooling. Due to the neglect of pressure adjustments, the geostrophic vorticity is stationary in time.

The roots (40.b) and (40.c) are damped inertial oscillations which result from an initial imbalance between the pressure gradient force, Coriolis, and frictional forces. The root (40.c) is not applicable to geophysical flows; it is a mathematical result corresponding to a negative rotation rate. The trajectory curvature resulting from inertial forces is anticyclonic, or clockwise in the Northern Hemisphere as in the root (40.b). Friction enhances trajectory curvature and frequency and modifies the kinetic energy of the flow through downward momentum transport as in Mahrt (1974). As in (40.a), the pressure field and geostrophic vorticity are stationary in time.

The higher order corrections are obtained through a set of recursion equations generated by a succession of limits ($\hat{B} \to 0$) applied to the expanded polynomial. The first two corrections to the zeroth order root $\alpha_o=0$ are as follows:

$$\alpha_1 = \frac{-\hat{C}_D \cos\eta}{(1+\hat{C}_D \sin\eta)^2 + (\hat{C}_D \cos\eta)^2} \tag{41}$$

$$\alpha_2 = \frac{-\hat{C}_D \cos\eta(2\alpha_1^2 + A^2) + \alpha_1}{(1+\hat{C}_D \sin\eta)^2 + (\hat{C}_D \cos\eta)^2} \tag{42}$$

The correction (41) represents order $\hat{B}$ pressure adjustments generated in the free flow and imposed upon the boundary layer. The time scale associated with the spin-down of an initial disturbance (e^{-1} folding time) to this order is

$$T_d \cong -(\hat{B}\,\alpha_1\,f)^{-1} = \frac{L}{hN_f}\left[\frac{(1+\hat{C}_D \sin\eta)^2 + (\hat{C}_D \cos\eta)^2}{\hat{C}_D \cos\eta}\right] \tag{43}$$

Within this time, an initial disturbance will loose most of its kinetic energy through conversion to available potential energy associated with adiabatic cooling in the free layer. To first order, pressure adjustments in the boundary layer do not enter the problem. The same time scale was obtained by Mahrt and Park (1976), who studied spin-down in the stratified flow above a neutral boundary layer.

The order $\hat{B}^2$ correction, (42), includes the effect of pressure adjustments within the boundary layer, as well as order $\hat{B}^2$ pressure adjustments aloft. This correction makes the estimate for $\hat{\alpha}$ more negative, which

shortens the spin-down time. The decreased lifetime of an initial disturbance can be attributed to pressure adjustments in the boundary layer as well as aloft.

Higher order corrections do not introduce any new physical mechanisms, and are negligibly small compared to the second order result if $\hat{B} << 1$.

The first order correction to the damped inertial oscillation $\alpha_o = - \hat{C}_D \cos\eta - i (1 + \hat{C}_D \sin\eta)$ is

$$\alpha_1 = - \frac{\sqrt{1 + \alpha_o^2}}{2\alpha_o} \qquad (44)$$

For any value of $\hat{C}_D$, the real part of α_1 is positive. The lifetime of the damped inertial oscillation is extended in the presence of the order $\hat{B}$ pressure adjustments in contrast to spin-down. The resulting weakening pressure gradient produces smaller accelerations, and thereby, a longer time scale for the decay of an initial disturbance.

IV. FORCED RESPONSE

Vertical motion forced directly by the surface heating in equation (21) is of the form,

$$w(h,t) = W(h)\, e^{-i\omega t} \tag{45}$$

where $W(h)$ is the unknown complex amplitude and ω is the specified forcing frequency. Substituting this expression into equation (26), and using the frictionless flow equations (32) and (33), leads to the following expression for the forced response:

$$W(h) = \frac{gQ_o(1-G)^{-1}}{(r+1)N_f L\theta_o\sqrt{f^2-\omega^2}} \tag{46}$$

where

$$G \equiv \frac{i\omega L}{hN_f\sqrt{f^2-\omega^2}}\left[\frac{C_D V}{h}\cos\eta - i\omega + \left(f + \frac{C_D V}{h}\sin\eta\right)^2\left(\frac{C_D V}{h}\cos\eta - i\omega\right)^{-1} + i\,\frac{h^2}{L^2}\,\frac{s}{(s+1)(r+1)}\,\frac{N_B^2}{\omega}\right]$$

This result indicates that the vertical motion amplitude is directly proportional to differential surface heating, Q_o/L, or equivalently, the generation of available potential energy. Stratification in the frictionless flow and the boundary layer inhibit vertical motion as in the steady-limit (Stommel and Veronis, 1957). On the other hand, accelerations may act against the constraining effect of rotation on cross-isobar flow and thus, enhance boundary layer production of vertical motion.

The solution is finite at the classical critical latitude unlike the classical Ekman solution (Holton et al., 1971) in which case both the boundary layer depth and vertical motion are singular as f approaches ω. Here the boundary layer depth is specified, as in Chang (1973).

In order to generalize the influence of the different variables, we will characterize the vertical motion response in terms of certain non-dimensional parameters. The following examples are just a few of many possible ways of framing the behavior of the response function.

A. Variation in Vertical Motion with Latitude

We first examine the dependence of boundary layer vertical motion on latitude for fixed forcing frequency, ω, by using the following form of equation (46)

$$\hat{w} \equiv W(h) \frac{(r+1)N_f L\, \theta_o \omega}{g\, Q_o} \tag{47}$$

$$= \left[\sqrt{f^{*2}-1} - \frac{i}{B^*} \left\{ (C_D^* \cos\eta - i) \left[1 + \left(\frac{f^* + C_D^* \sin\eta}{C_D^* \cos\eta - i} \right)^2 \right] + iA^2 B^{*2} \right\} \right]^{-1}$$

where:

$f^* \equiv f/\omega$ = scaled latitude

$$B^* \equiv \frac{hN_f}{L\omega} f = f^* \hat{B}$$

$$C_D^* \equiv \frac{C_D V}{h\omega} = f^* \hat{C}_D$$

$$A \equiv \sqrt{\frac{s}{(s+1)(r+1)}}\ \frac{N_B}{N_f}$$

For diurnal variations ω is approximately $.7 \times 10^{-4}$ sec^{-1}. Then $f^* \sim 1.4$ corresponds to a midlatitude value, 45° N, and $f^* \sim 1.0$ to 30°N, the critical latitude for diurnal forcing. The complex number $\hat{w}$ is vertical motion normalized by the scale velocity

$$W_s = \frac{g\, Q_o}{(r+1)\, N_f L\, \theta_o \omega} \tag{48}$$

i) Vertical Motion Response Magnitude

In figures 1 and 2 the normalized real magnitude is plotted against the non-dimensional latitude, f^* for various values of B^* and C^*_D in a stratified boundary layer with A = 1. The peaks in both figures are shifted equatorward of the classical critical latitude $f^* = 1$, in contrast to the classical Ekman result. In this model, maximum convergence occurs at the latitude in which the natural frequency of the unforced mode matches the forcing frequency, for the specified values of B^*, C^*_D, A, and n.

From the theory of internal gravity waves, it is well known that an increase in stratification or aspect ratio increases the frequency of inertial-gravity oscillations (Eckart, 1960). The natural frequency of a frictionless inertial-gravity wave in a Boussinesq atmosphere is

$$\omega_n^2 = f^2 + (k_H/k_3)^2\, N_f^2 \tag{49}$$

$$= f^2 + (ch/L)^2\, N_f^2$$

where k_H and k_3 are horizontal and vertical wave numbers, and $c \equiv (hk_3)^{-1}$. Since the boundary layer vertical structure has been integrated, c is unknown. Dividing by ω^2 leads to an expression for the "resonant" latitude f^*_r, the latitude at which the forcing frequency matches the natural

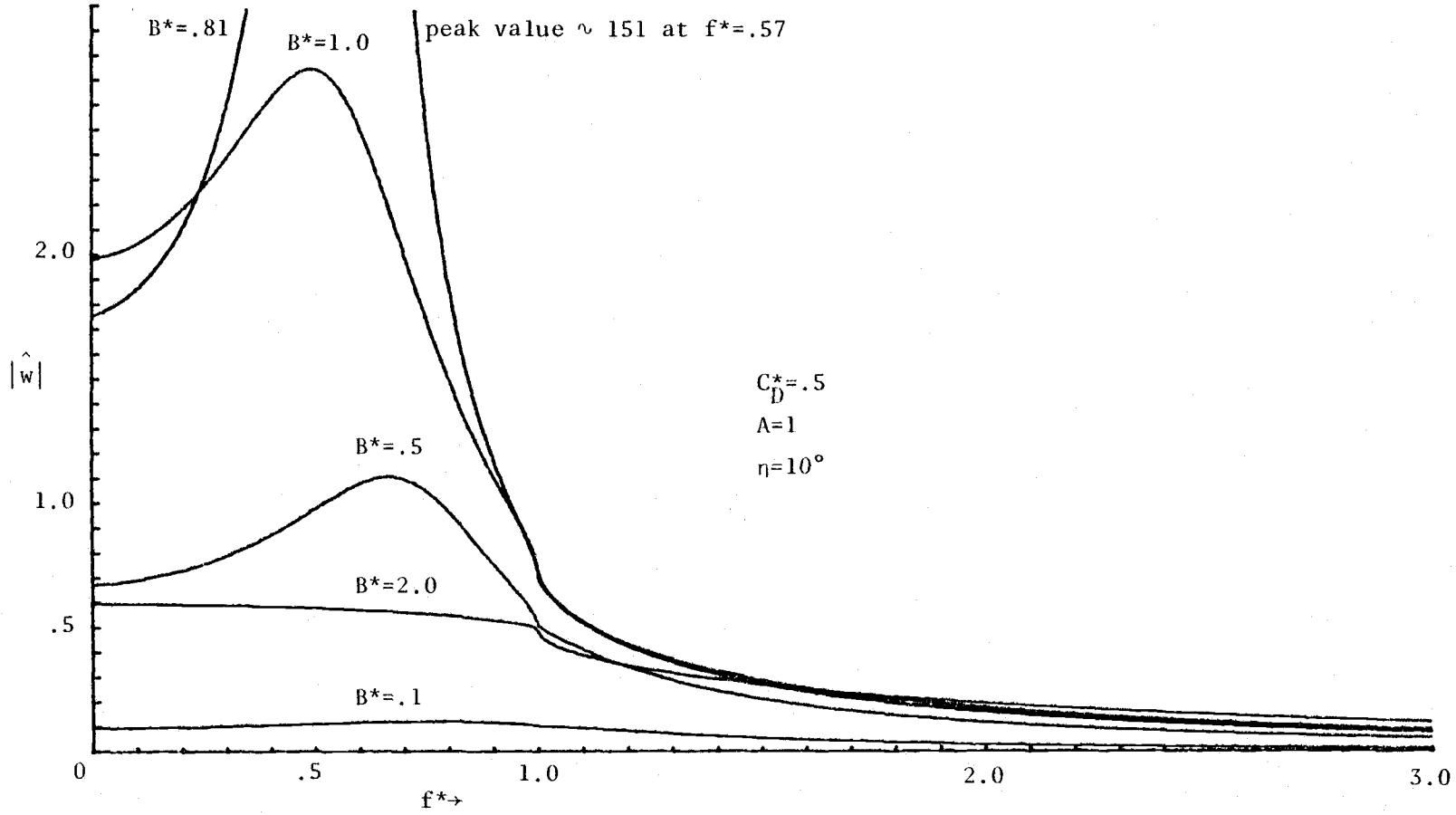

Fig.1. Scaled magnitude of the vertical velocity (equation (47)) as a function of scaled latitude for several different values of B*, with C_D^* = .5, A = 1, η = 10 degrees.

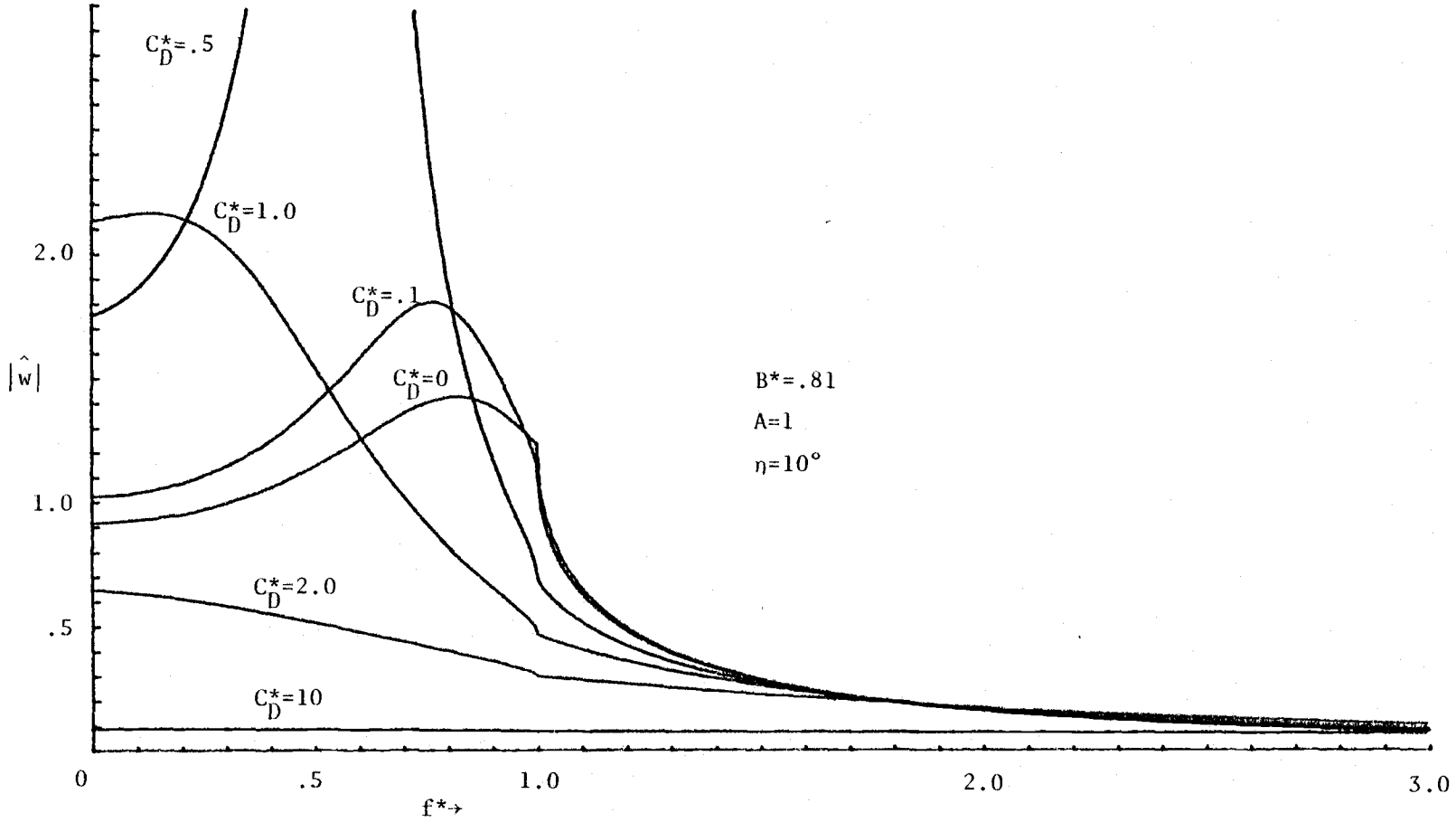

Fig. 2. As in Fig. 1. except for several different values of C_D^*, with B* = .81, A = 1, η = 10 degrees.

frequency of the frictionless inertial-gravity oscillation.

$$(\omega_n/\omega)^2 = 1 = f_r^{*2} + c^2 B^{*2} \tag{50}$$

or

$$f_r^{*2} = 1 - c^2 B^{*2}$$

Thus, the greater the stratification or the smaller the horizontal length scale the greater the equatorward shift of the critical latitude.

Although traveling wave solutions are not allowed in our model, the scale arguments which lead to equation (50) can be justified under a more complete representation of the free modes. In figure 1 the equatorward shift increases with B* although friction and boundary layer pressure adjustments further complicate the problem.

The equatorward shift in figure 2, which increases with C^*_D, can be explained through the unforced mode calculations in the previous section. Neglecting pressure adjustments, the natural frequency of the friction-inertial oscillation from equation (40.b) is

$$\omega_n = -(f + \frac{C_D V}{h} \sin\eta) \tag{51}$$

Solving for the resonant latitude,

$$f^*_r = 1 - C^*_D \sin\eta \tag{52}$$

we obtain an equatorward shift which increases with C^*_D. In figure 2 with B* = .81, higher order effects due to stratification lead to a larger shift than predicted by equation (52).

The magnitude of the response at the resonant latitude in figure 1 increases with B* until some preferred value, approximately B* = .81. Further

increases in B* beyond this value reduce the maximum production of vertical motion. Since the scaling velocity W_s in equation (48) must remain fixed, we can consider only those variations of B* in which $N_f L$ is constant. Furthermore, if C^*_D is to remain fixed, we consider the case in which h is constant as well, resulting in the relation

$$B^* \propto L^{-2} \tag{53}$$

For B* small, L is large so that the surface heating and resulting convergence is spread out over a large horizontal scale. The vertical motion over the fixed depth h is proportionately small. Vertical motion increases as the heating and convergence is concentrated in a smaller horizontal scale. This enhancement continues until the opposing influences of adiabatic cooling and the resulting pressure adjustments, which are also strengthening as L is decreased, finally dominate as L becomes smaller than the preferred length scale L_p. That is over scales less than L_p, the concentration of convergence is secondary to the importance of strengthening of pressure adjustments which oppose vertical motion. The preferred length scale represents the scale over which a fixed amount of heating generates the strongest circulation. In figure 1 this scale is approximately

$$L_p = \frac{h N_f}{.81\omega} \approx 175 \text{ km}$$

where $\omega = .7 \times 10^{-4}$ sec^{-1} (diurnal), $N_f = 10^{-2}$ sec^{-1}, and h = 1 km. The largest peak is centered at f* = .57 or at 16.6°N latitude for diurnal forcing, and has a dimensional amplitude of 2.0 m sec^{-1} for significant forcing corresponding to $Q_o = 10^{-1}$ m sec^{-1} °K, with $\theta_o = 300$°K, and r=1. Under the same conditions, the midlatitude vertical motion is 4.0×10^{-3} m sec^{-1}.

In the neighborhood of the resonant peak, where the forced vertical motion is very large, non-linear terms, which were neglected in the basic equations, become important and the actual vertical motion magnitude may be greatly modified from the model prediction.

The resonant response in figure 2 varies with C_D^* in a manner analagous to B^* in figure 1. That is for small C_D^*, the peak response increases with C_D^* until a critical value, $C_D^* = .5$. Further increases reduce the response at the resonant latitude. This behavior, which is discussed by Mahrt (1974), is due to the two opposing influences of friction on cross-isobar flow. The surface stress simultaneously rotates the wind towards the pressure gradient and reduces the flow speed. For small C_D^* the increased cross-isobar component indicates that the drag primarily rotates the wind vector with less important reduction of wind speed. For $C_D^* \geq .5$ the decreasing flow speed exceeds the rotational effect and increased drag reduces the cross-isobar flow and convergence.

ii) Vertical Motion Response Phase

In figures 3 and 4 the phase of the response with respect to the forcing is plotted as a function of latitude for different values of B^* and C_D^*, respectively. The response lags the forcing by less than a quarter cycle poleward of the critical latitude, but equatorward the phase lag of the response is quite complicated.

Pressure adjustments due to vertical motions increases the adjustment rate of the flow and decreases the phase lag of the response. As B^* approaches infinity, due to vanishing horizontal length scale, the response becomes in phase with the forcing (figure 3) for all latitudes. For large $B^* >> f^*$, C_D^* adiabatic cooling due to vertical motion balances surface heating.

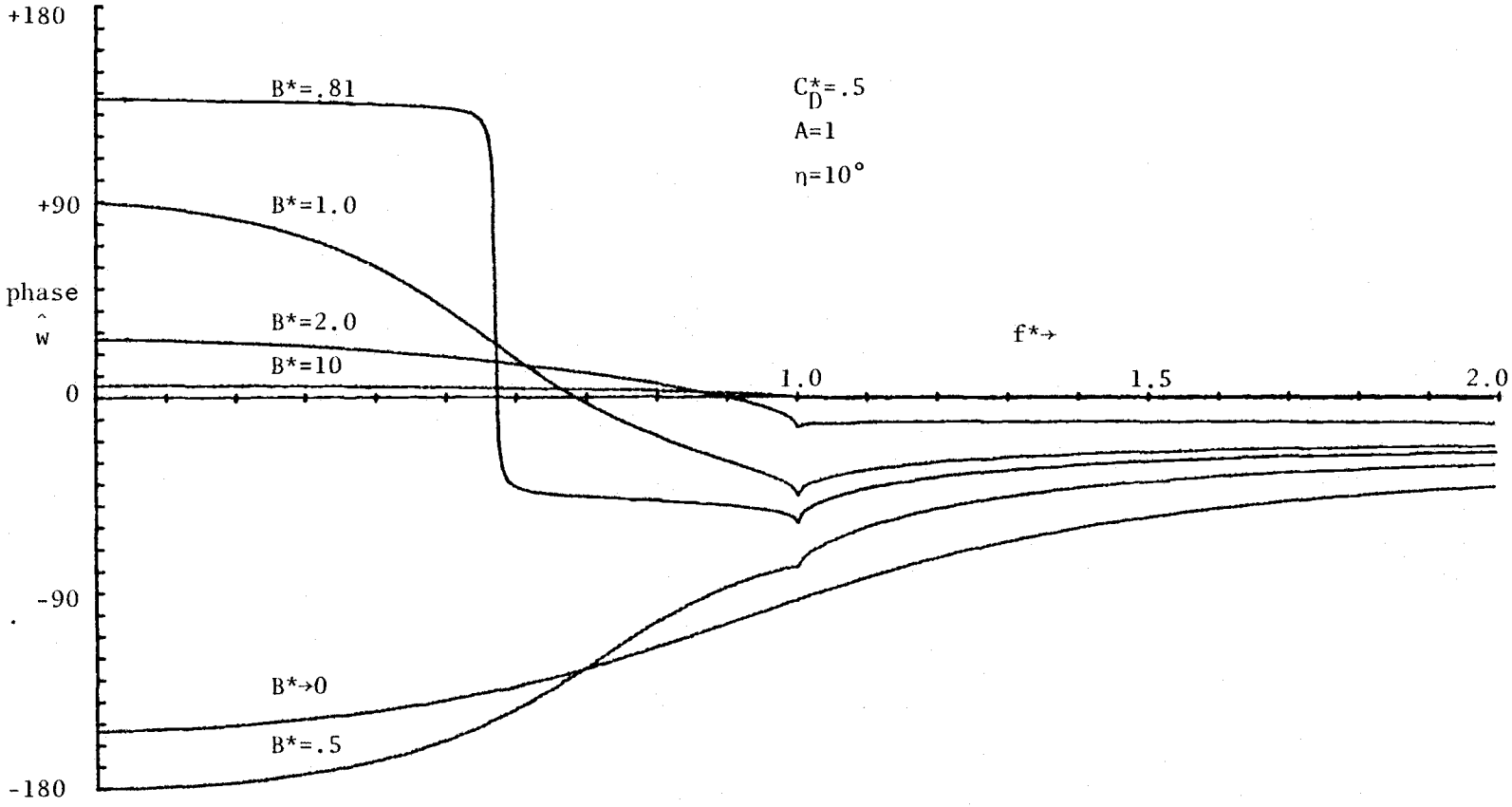

Fig. 3. Phase of vertical velocity (equation (47)) as a function of scaled latitude for several different values of B*, with C_D^* = .5, A = 1, η = 10 degrees.

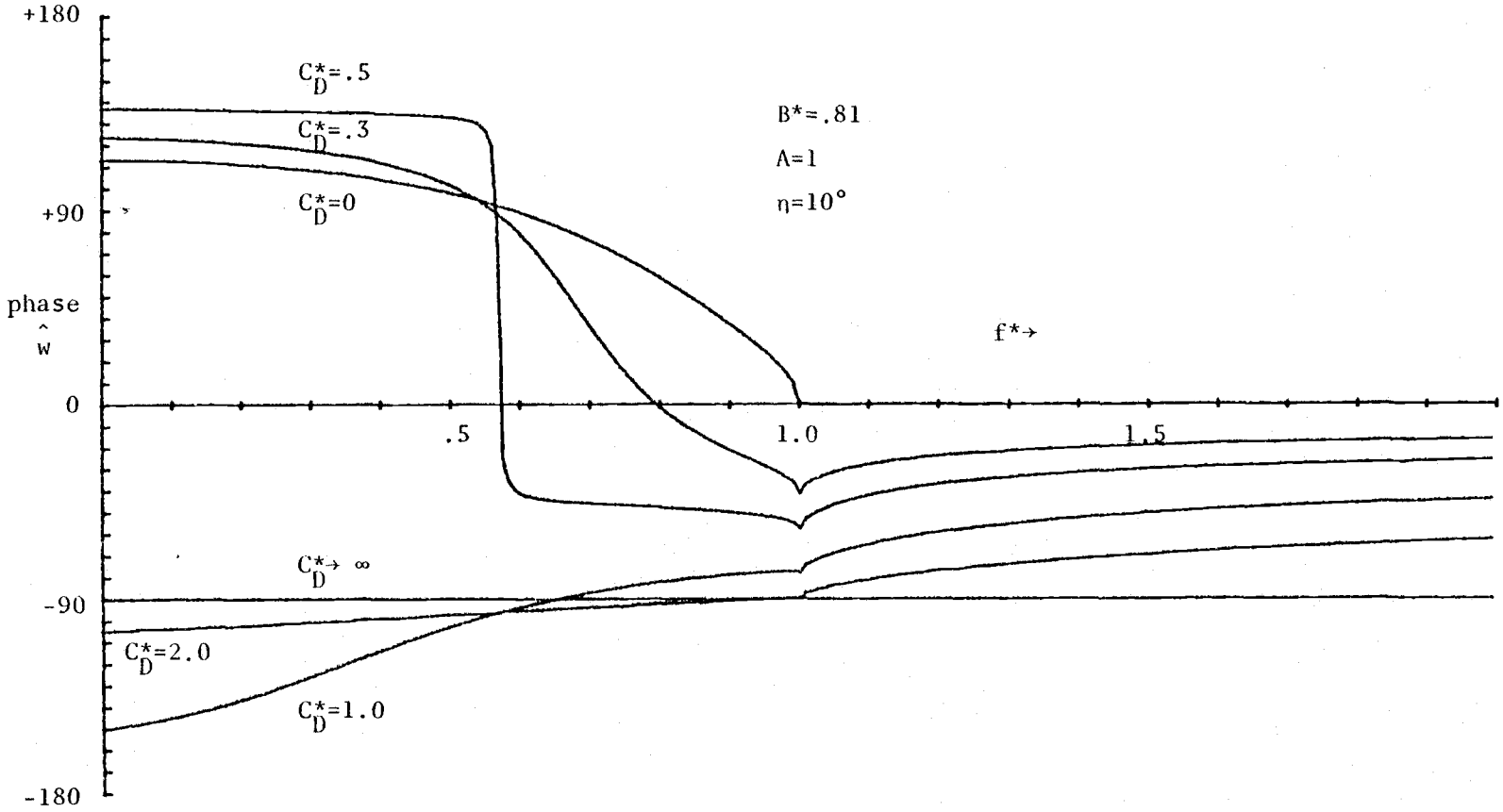

Fig. 4. As in Fig. 3. except for several different values of C_D^*, with B* = .81, A = 1, η = 10 degrees.

When pressure adjustments and accelerations are small and convergence is induced primarily through friction, as in classical Ekman pumping, vertical motion lags the forcing by a quarter cycle (figure 3). When f* and B^* are large, the phase is influenced by both the Ekman balance component of the flow and accelerations responding to pressure adjustments. Then lags are less than a quarter cycle. For diurnal-mid-latitude forcing, $f^* = 1.4$, and $B^* = .81$, the vertical motion lags the forcing by about two hours. At the same latitude and frequency, the lag increases to four hours for $B^* = .1$.

As C_D^* approaches infinity in figure 4, frictionally induced convergence dominates other effects as in the classical Ekman solution and vertical motion lags the forcing by a quarter cycle. For finite C_D^* the Ekman limit is approached by the less restrictive conditions:

$$f^*, C_D^* >> 1 \qquad \text{and} \qquad B^* << f^*, C_D^*$$

At the resonant latitude, $f^* = .57$, there is a 180° phase shift under resonant conditions $B^* = .81$, $C_D^* = .5$ in figures 3 and 4. This shift is discussed by Holton et al. (1971) for the Ekman layer solution (constant eddy viscosity) and is analagous to the phase shift for resonant forcing of a damped harmonic oscillator (Feynman, 1964).

B. Variation in Vertical Motion with Stratification Parameter

Using equation (47) with f^*, C_D^*, and A fixed, we can characterize the response as a function of B^*. The vertical motion is again scaled according to W_s in equation (48) so that ω, N_f, and h are considered to be fixed.

In figure 5 the scaled vertical motion magnitude is plotted for various scaled latitudes from $f^* = 0$ (equator) to $f^* = 10$ (synoptic frequencies at high latitudes). The preferred value of B^*, for which vertical motion is a maximum, is smallest (largest length scale) at the resonant latitude, $f_r^* = .57$. At this latitude rotation opposed by accelerations and adiabatic pressure adjustments are least effective in constraining the vertical motion (for fixed ω, N_f, N_B, C_D^*, and h). Away from the resonant latitude, the maximum response for a given surface heating occurs at smaller scales; hence, the preferred value for B^* increases. For diurnal-mid-latitude forcing, $f^* = 1.4$, the preferred value $B^* = 1.2$ corresponds to a preferred length scale $L_p = 120$ km, for $N_f = 10^{-2}$ sec^{-1} and h = 1 km. For a typical nocturnal boundary layer when h = 200 m and $N_f = 2 \times 10^{-2}$ sec^{-1}, L_p is 48 km.

Figure 6 exhibits the influence of boundary layer stratification on the preferred B^* value for $f^* = 1.4$ and $C_D^* = .5$. In a neutral boundary layer (A=0), vertical motion increases indefinitely with B^*. That is without adiabatic pressure adjustments in the boundary layer, convergence is maximized in the limit $L \to 0$. In this case, as in classical Ekman pumping, decreasing L serves only to concentrate convergence and to enhance vertical motion. As the boundary layer stratification is increased (A>0), the preferred length scale increases as adiabatic pressure adjustments effectively reduce vertical motion production at small scales. For A = .1, the preferred B^* is 1. If we take $N_f = 10^{-2}$ sec^{-1}, h = 1 km, (r,s) = 1, and the diurnal frequency, the former case corresponds to daytime conditions.

$$N_B = A N_f \sqrt{\frac{(s+1)(r+1)}{s}} = .2 \times 10^{-2} \text{ sec}^{-1}$$

$$L_p = \frac{h N_f}{B_p^* \omega} = 14 \text{ km}$$

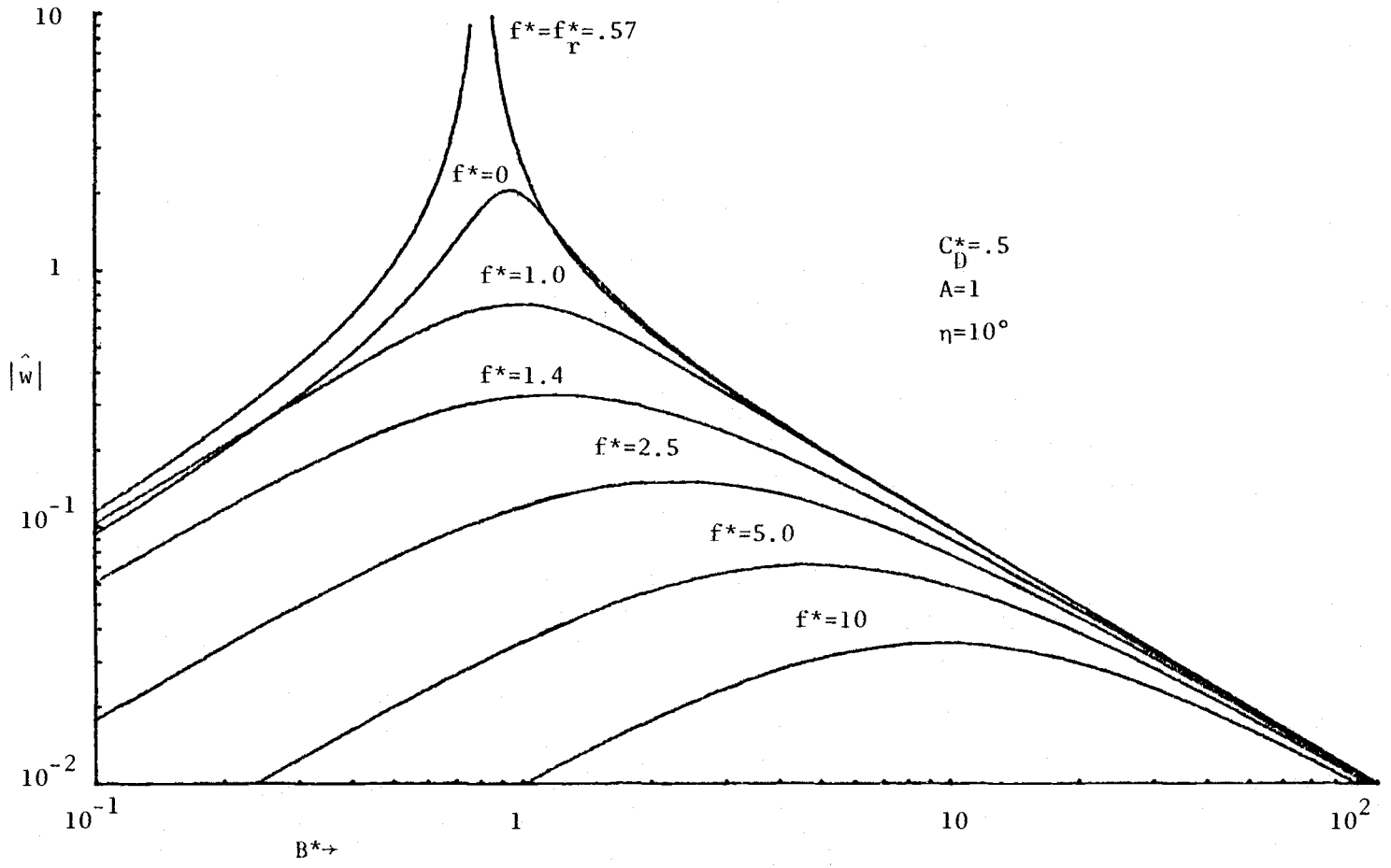

Fig. 5. Scaled magnitude of the vertical velocity (equation (47)) as a function of stratification parameter for several different values of f*, with C_D^*=.5, A = 1, η = 10 degrees.

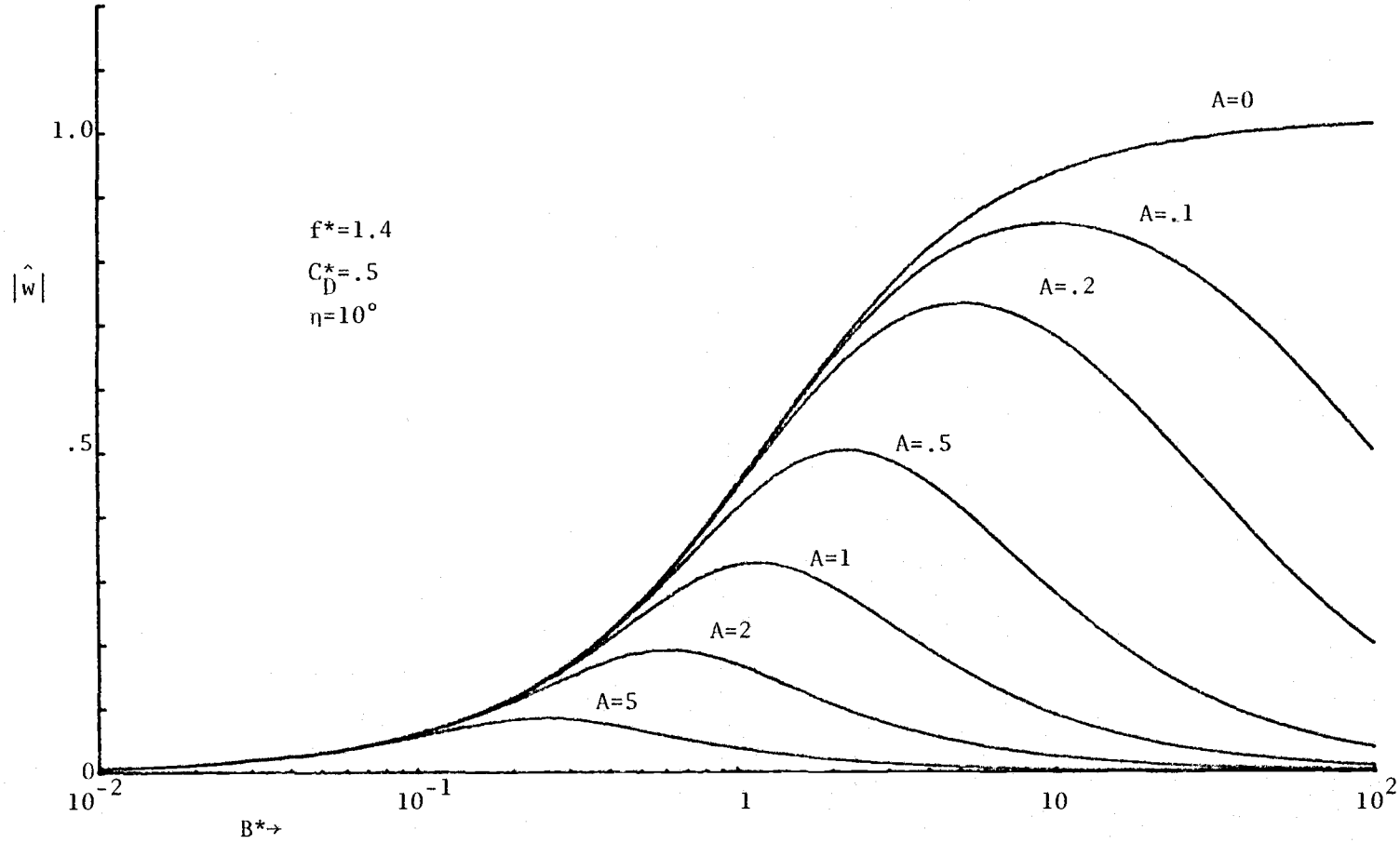

Fig. 6. As in Fig. 5. except for several different values of A with f* = 1.4, C_D^* = .5, η = 10 degrees.

and the latter to typical night-time conditions

$$N_B = 2 \times 10^{-2} \text{ sec}^{-1}$$

$$L_p = 140 \text{ km.}$$

C. Variation in Vertical Motion with Friction Parameter

Figure 7 shows how the scaled vertical motion amplitude varies with C_D^* at various scaled latitudes for $B^* = .81$. The curves are similar to those in figure 5. The maximum response for each latitude occurs at some critical value of C_D^*. For $f^* \sim 1.0$, the response is largest at $C_D^* = 0$ ($C_D^* = 0$ is beyond the lower limit of the log scale in figure 7). Then frictional drag acts only to inhibit convergence by reducing the total flow and cross-isobar flow. Away from $f^* = 1.0$, friction enhances cross-isobar flow and convergence by rotating the wind ($C_D^* < C_D^*$ critical) and inhibits convergence through drag on the total flow ($C_D^* > C_D^*$ critical) in agreement with discussions in Sec. II-A.

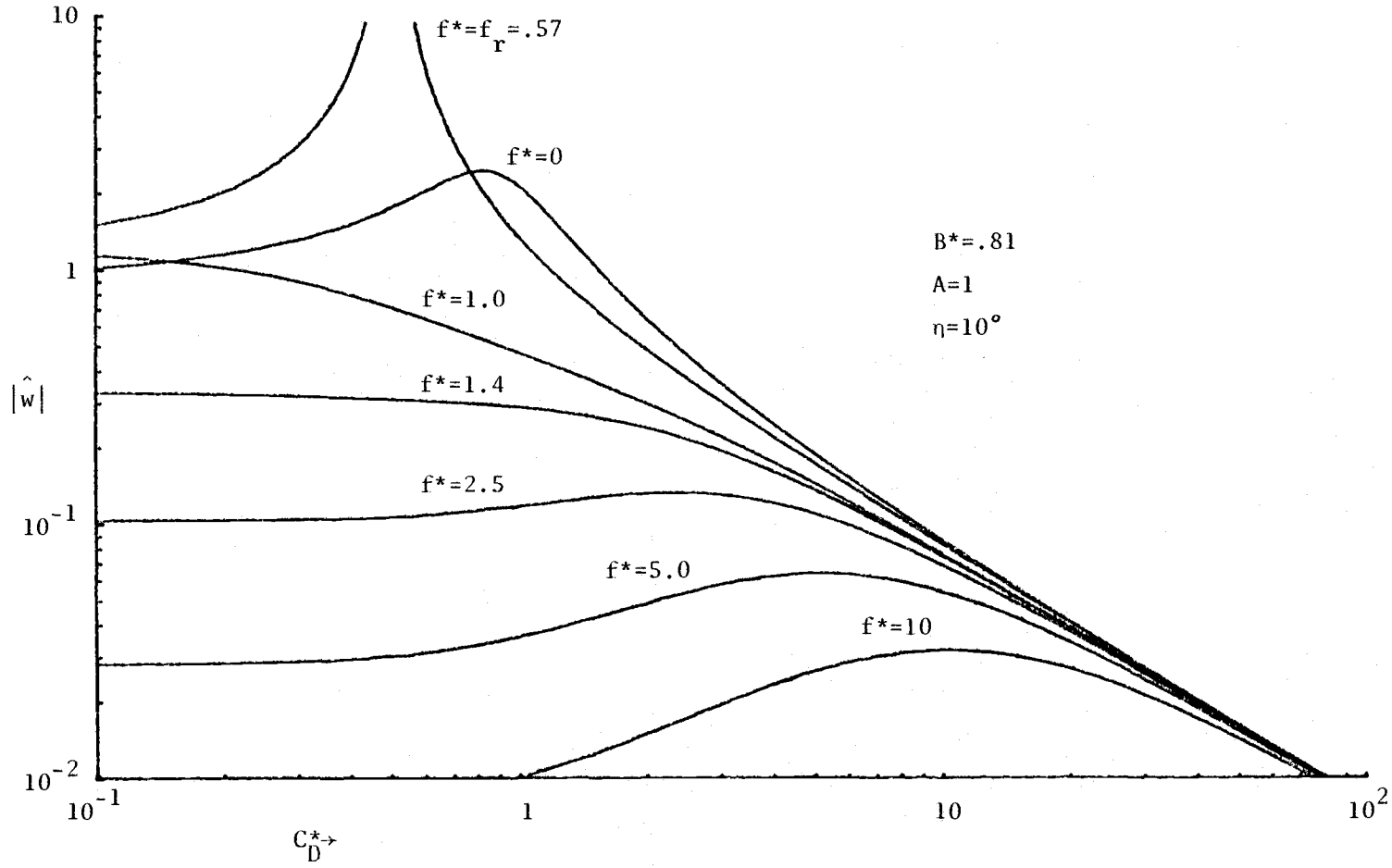

Fig.7. Scaled magnitude of the vertical velocity (equation (47)) as a function of the scaled drag coefficient for several different values of f*, with B* = .81, A = 1, η = 10 degrees.

V. CONCLUSIONS AND FURTHER DISCUSSION

Although the geophysical boundary layer is much more complicated than the analytical treatment presented here, we can formulate some general expectations that can be applied to certain naturally occurring atmospheric phenomena. The present development is an improvement upon previous analytical developments in that the assumption of an eddy viscosity is eliminated and stratification in the boundary layer is included.

For example, based on the results of the simplified two-layer model we expect significant variation of vertical motion with latitude for convergence forced by a time-dependent, oscillating surface heat flux. The maximum vertical motion occurs at a resonant latitude where natural modes of oscillation in the boundary layer have the same frequency as the forcing. These natural modes are influenced by both the frictionless dynamics and turbulent transport of heat and momentum. The resulting critical latitude is equatorward from the classical critical latitude associated with Ekman pumping.

In the presence of low-level stratification, we expect the smallest scales of motion to be damped out by pressure adjustments. The larger scales are ineffective in concentrating convergence. The intermediate preferred scale of maximum response increases with boundary layer stratification and decreases with distance from the resonant latitude.

Here we study physical mechanisms which will be important in actual geophysical flows along with other mechanisms omitted in the present study. Here the flow is forced by differential heating. This type of forcing contributes to diurnal geophysical flows such as the sea-breeze

circulations prevalent in coastal regions and thermal tidal winds in, for example, the Great Plains (MacKay, 1971).

Since nonlinear advections are important in most sea-breeze circulations, the present study identifies only one aspect of such circulations. The observed sea-breeze circulations reach their maximum strength from two to five hours after the maximum land-sea temperature difference (Gutman, 1972). In the present model, this range of phase lags between thermal structure and the wind speed could be explained through typical variations in atmospheric conditions (B^*, C_D^*) for mid-latitude flows, as depicted in figures 4 and 5.

Many authors have studied the critical latitude effect and its relationship to observed cloud and precipitation patterns. Some investigators feel that diurnal variations in surface stress and heat flux associated with buoyancy effects along sloped terrain are responsible for the initiation of nocturnal thunderstorms in the Great Plains region. This type of mechanism is supported by observational evidence (Wallace, 1975) indicating the importance of the diurnal cycle in modulating thunderstorm activity. Paegle and Rasch (1973) show that vorticity advection could shift the maximum vertical velocity poleward from the classical diurnal critical latitude (30°N) into the Central Great Plains region. In the present study, we have considered the influence of stratification, drag coefficient, boundary layer depth, and the horizontal scale and frequency of the forcing on the critical latitude through the non-dimensional parameters B^* and C_D^* . The influence of these parameters is to shift the critical latitude equatorward which

suggests that the nocturnal Great Plains thunderstorms are not associated with the critical latitude effects presented here. However the present model is an improvement on previous models in that pressure adjustments and a more realistic parameterization of friction is included here.

Model applicability could be further improved by including the diurnal variation of boundary layer depth, drag coefficient, and stratification. The collapse of the daytime mixed layer into a shallower stably stratified nocturnal boundary layer involves significant variations of h, C_D, and N.

Much attention has been directed toward the synoptic scale critical latitude near 5° to 10° N and S, which is believed to play an important role in the development of the intertropical convergence zone (ITCZ). Studies of this type (Holton et al., 1971; Chang, 1973; Kuo, 1975) are forced by a specified synoptic scale pressure field associated with equatorial wave disturbances. The present study could be extended to include this type of forcing by imposing a specified pressure field at the free flow top. The equatorward shift of the critical latitude in the present model forced by surface heating contrasts to earlier results with specified pressure fields (Chang, 1973; Kuo, 1975) which predict a poleward shift from the classical synoptic scale critical latitude (Holton et al., 1971). In the present model, the location of the maximum vertical motion is dependent on various atmospheric conditions through their influence on the natural modes of oscillation in the boundary layer.

BIBLIOGRAPHY

Barcilon, V., and J. Pedlosky, 1967: Linear theory of rotating stratified fluid motion. J. Fluid Mech., 29, 1-16.

Chang, C.P., 1973: On the depth of the equatorial boundary layer. J. Atmos. Sci., 30, 436-443.

Charney, J.G., and A. Eliassen, 1949: A numerical method of predicting the pertubations of the middle latitude westerlies. Tellus, 1, 38-54.

Eckart, C., 1960: Hydrodynamics of Oceans and Atmospheres. Pergamon Press, New York, 290 pp.

Feynman, R.P., 1964: The Feynman Lectures on Physics. Vol. 1. Addison-Wesley, Reading, Mass., 538 pp.

Geisler, J.E., and E.B. Kraus, 1969: The well-mixed Ekman boundary layer. Deep-Sea Res., 16, Suppl., 73-84.

Greenspan, H.P., 1968: The Theory of Rotating Fluids. Cambridge University Press, London, 327 pp.

_____, and L.N., Howard, 1963: On the time-dependent motion of a rotating fluid. J. Fluid Mech., 17, 385-404.

Gutman, L.N., 1972: Introduction to the Nonlinear Theory of Mesoscale Meteorological Processes. Israel Program for Scientific Translations, Jerusalem, 224pp.

Holton, J.R., 1965: The influence of viscous boundary layers on transient motions in a stratified rotating fluid. Part I. J. Atmos. Sci., 22, 402-411.

_____, J.M. Wallace and J.A. Young, 1971: On boundary layer dynamics and the ITCZ. J. Atmos. Sci., 28, 275-280.

Kuo, H.L., 1973: Planetary boundary layer flow of a stable atmosphere over the globe. J. Atmos. Sci., 30, 53-65.

_____, 1975: Planetary boundary layer of equatorial waves and critical latitude. Bound. Layer Meteor., 9, 163-190.

Lavoie, R., 1972: A mesoscale numerical model of lake-effect storms. J. Atmos. Sci., 29, 1025-1040.

Leetmaa, A., 1971: Some effects of stratification on rotating fluids. J. Atmos. Sci., 28, 65-71.

Mahrt, L. J., 1974: Time-dependent integrated planetary boundary layer flow. J. Atmos. Sci., 31, 457-464.

_____, and S. U. Park, 1976: The influence of boundary layer pumping on synoptic-scale flow. J. Atmos. Sci., 33, 1505-1520.

MacKay, K. P., Jr., 1971: Steady state hodographs in a baroclinic boundary layer. Bound. Layer. Meteor., 2. 161-168.

Paegle, J., and G. Rasch, 1973: Three-dimensional characteristics of diurnally varying boundary-layer flows. Mon. Wea. Rev., 101, 746-756.

Park, S. U., and L. J. Mahrt, 1978: Oscillating stratified boundary layers. Submitted to Tellus.

Stommel, H., and G. Veronis, 1957: Steady convective motion in a horizontal layer of fluid heated uniformly from above and cooled non-uniformly from below. Tellus, 9, 401-407.

Wallace, J. M., 1975: Diurnal variations in precipitation and thunderstorm frequency over the conterminous United States. Mon. Wea. Rev., 103, 406-419.

Young, J. A., 1973: Isallobaric air flow in the planetary boundary layer. J. Atmos. Sci., 30, 1584-1592.